Evolution of (001) and (111) facets for selective epitaxial growth inside submicron trenches

S. Jiang, C. Merckling, W. Guo, N. Waldron, M. Caymax, W. Vandervorst, M. Seefeldt, and M. Heyns

Citation: Journal of Applied Physics **115**, 023517 (2014);
View online: https://doi.org/10.1063/1.4861416
View Table of Contents: http://aip.scitation.org/toc/jap/115/2
Published by the American Institute of Physics

Evolution of (001) and (111) facets for selective epitaxial growth inside submicron trenches

S. Jiang,[1,2,a)] C. Merckling,[1] W. Guo,[1] N. Waldron,[1] M. Caymax,[1] W. Vandervorst,[1,3] M. Seefeldt,[2] and M. Heyns[1,2,b)]
[1]*IMEC, Kapeldreef 75, B-3001 Heverlee, Belgium*
[2]*Department of Metallurgy and Materials Engineering, KULeuven, Kasteelpark Arenberg 44-bus 2450, B-3001 Heverlee, Belgium*
[3]*Department of Physics and Astronomy, KULeuven, Celestijnenlaan 200D-bus 2418, B-3001 Heverlee, Belgium*

(Received 30 October 2013; accepted 20 December 2013; published online 13 January 2014)

The evolution of (001) and (111) facets for the epitaxial growth inside submicron trenches is systematically studied in this report. The analysis with the method of "Lagrange multiplier" indicates the equilibrium crystal shape. In the case of non-equilibrium without external fluxes, we employed the "weighted mean curvature" method to mathematically model the inter-facet migration rate for two extreme kinetic cases: "surface diffusion limited" and "surface attachment/detachment limited." Coupled with external supply of atoms, the self-limited behavior of facet size is theoretically predicted. Moreover, we find that the self-limited stable facet size in trenches of different widths has a specific relationship determined by the surface energy ratio, kinetic rate ratio, and isolated growth rate difference. The two limited cases could be discriminated according to the mathematical fitting of one exponent in this relationship based on the stable facet size in trenches of different widths. © *2014 AIP Publishing LLC*. [http://dx.doi.org/10.1063/1.4861416]

I. INTRODUCTION

The facet evolution is of great interests for the research of epitaxial growth. It primarily influences the final morphology, particularly of the island growth mode, for practical applications. Moreover, the investigation of facet evolution would acquire the insightful information of surface energies and kinetics, which are theoretical foundations and guidelines for epitaxy. In the occasion of selective growth on (001) oriented surface, due to the interfacial energy with the sidewall, even for homoepitaxy (e.g., Si on Si,[1,2] as well as heteroepitaxy, SiGe on Si,[3] InP on Si[4,5]) extra facets, such as (311) or (111) will generate close to the sidewall in order to minimize the total surface energy. Afterwards, these facets will develop in specific growth rate (GR), which influences the crystal shape. Extensive experimental study about the GR of individual facet can be found in the literatures, see Refs. 3 and 6. For patterned substrates in micrometer scale, there are several models proposed to understand the facet GR and final crystal morphology, also including inter-facet surface diffusion (SD), e.g., Refs. 6–14. However, detailed understanding of submicron scale trench features, including interfacial energy with sidewalls and surface kinetics, is not available yet for the selective growth of semiconductors.

In this review, we utilize the selective growth behavior of III-V materials as an example, in order to systematically study the facet evolution inside submicron trenches from equilibrium case to non-equilibrium one. However, we believe the developed models should be applicable for other material system with similar facets. In Sec. II, the facet formation (e.g., mostly (001) and (111) facets according to the experimental observation) in equilibrium is firstly analyzed with the method of Lagrange multiplier. It is theoretically concluded that the ratio of facet size can be the criteria of equilibrium in variant trench width. Then in Sec. III, the inter-facet migration for the case of non-equilibrium shape (ES) firstly without external supply of atoms is investigated in the framework of "weighted mean curvature" (WMC) pioneered by Carter[13] and Taylor[15,16] for both surface diffusion limited and surface attachment/detachment limited processes. The surface chemical potential and the growth/recess rate of (001) and (111) facets of dimension dependence are explicitly illustrated. Coupled with the external supply flux rate as in the growth experiments, the self-limited behavior is theoretically analyzed and the correlation of stabilized facet size with the trench width, kinetic coefficient ratio, and external supply rate is mathematically described. It could be potentially employed to assess the predominant process, i.e., surface diffusion or surface attachment/detachment. Finally, the conclusion will be given in Sec. IV.

II. EQUILIBRIUM CRYSTAL SHAPE

Normally, due to the lattice mismatch of III-V materials with Si substrates, the first step is a low temperature nucleation/buffer layer. The migration of adatoms could be prohibited so the minimum energy state cannot be reached readily. Additionally, a significant amount of defects are concentrated in the layer at the bottom of trenches, which can influence the evolution of facets in this stage. Therefore, our discussion will be focused on the facet evolution in the mid-range of trenches. Due to the trapping effects, the extended defect density is reasonably low.[5] We employed the method

a)Electronic mail: jiang@imec.be.
b)Electronic mail: marc.heyns@imec.be.

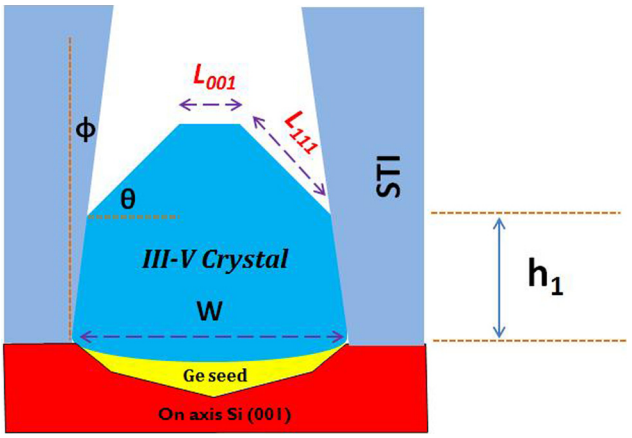

FIG. 1. Schematic of III-V SEG growth inside submicron STI trenches on on-axis (001) Si substrates, (111) and (001) facets commonly observed.

of Lagrange multipliers to deduce the size of each commonly observed facets (i.e., (001) and (111) facets in Fig. 1) minimizing the total surface energy for certain volume of deposited materials. It should be noted that the strain energy is not considered. The analysis will be treated as a two dimensional issue since the longitudinal size of crystal is significantly larger than the width for long sub-micron STI (shallow trench isolation) trenches. The sidewall material is eHARP (enhanced high aspect ratio process) silicon oxide. The typical growth procedure refers to Refs. 4 and 5.

Following the standard procedure of the method of Lagrange multiplier, if there is a tapering angle φ of STI sidewall, the total surface area in Fig. 1 can be computed as

$$S = (W - h_1\tan\phi)h_1 + \frac{1}{4}[(W - 2h_1\tan\phi)^2 - {L_{001}}^2]\tan\theta. \tag{1}$$

The total surface energy without taking the interface between the III-V solid and Ge buffer into consideration since it will be constant for this analysis,

$$E_s = 2(\gamma_{\mathrm{IIIV}-sidewall} - \gamma_{sidewall})\frac{h_1}{\cos\phi} + \frac{(W - 2h_1\tan\phi) - L_{001}}{\cos\theta}\gamma_{111} + L_{001}\gamma_{001}, \tag{2}$$

where, γ_{001}, γ_{111}, $\gamma_{\mathrm{IIIV}\text{-}sidewall}$ and $\gamma_{sidewall}$ are the specific surface energy for Facet (001), Facet (111), IIIV-*sidewall* interface and sidewall respectively.

In order to find the conditions for the minimum of E_s with the fixed value of S, by employing the method of Lagrange multiplier (λ is the multiplier), we obtained

$$L(h_1, L_{001}, \lambda) = E_s + \lambda\left\{(W - h_1\tan\phi)h_1 + \frac{1}{4}[(W - 2h_1\tan\phi)^2 - {L_{001}}^2]\tan\theta - S\right\}. \tag{3}$$

By equating the first derivative to zero, the value of (001) facet size for the minimum energy state should satisfy the following relation:

$$L_{001}(\text{minimum}) = \frac{\left(\frac{\gamma_{111}}{\cos\theta} - \gamma_{001}\right)\cot\theta}{\frac{\gamma_{\mathrm{IIIV}-sidewall} - \gamma_{sidewall}}{\cos\phi} - \frac{\gamma_{111}\tan\phi}{\cos\theta}} \times [(W - 2h_1\tan\phi)(1 - \tan\phi\tan\theta)]. \tag{4}$$

Additionally, if the sidewall is straight, $\phi = 0$,

$$L_{001}(\text{minimum}) = \frac{\left(\frac{\gamma_{111}}{\cos\theta} - \gamma_{001}\right)\cot\theta}{\gamma_{\mathrm{IIIV}-sidewall} - \gamma_{sidewall}}W. \tag{5}$$

As indicated by the equation, at the minimum total surface energy state, the width of (001) (if there is only (001) facet on the top) reaches the minimum value (non-zero) and this value is proportional to $[(W - 2h_1\tan\phi)(1 - \tan\phi\tan\theta)]$ in these nano-trenches. In this state, the facet (001) and (111) reaches the equivalent surface chemical potential (we notice that the interface chemical potential needs more investigation, which is beyond the scope of this report). Energetically, the replacement of (001) facet by (111) facet increases the surface energy, otherwise, for the homo-epitaxy on (001) substrates, pyramids rather than smooth growth front would be frequently observed. However, inside trenches, due to the interfacial energy between crystal and oxide sidewall, the formation of (111) facet can lower the contact area of the interface with the sidewall.[1,2] Therefore, the compromise of these two effects determines the specific crystal shape inside trenches. The quantitative description of equilibrium facet size demands the accurate information of surface/interface energies. However, practically the equilibrium crystal shape is rather difficult to be realized due to the far-from equilibrium characteristics of metalorganic vapor phase epitaxy (MOVPE) growth. It would be approaching to the equilibrium shape if the supplying rate is sufficiently low and surface temperature is sufficiently high. In order to further investigate the facet evolution, the kinetic process should be assessed. Therefore, the "WMC" method has been employed to analyze the influence of surface/interface energy coupled with surface kinetics on the growth rate of individual facet in Sec. III.

III. "WEIGHTED MEAN CURVATURE" METHOD ANALYSIS

The crystal equilibrium shape during the growth is rarely realized, consequently there will be a gradient of surface chemical potential to drive the mass flux to approach the equilibrium shape.[17,18] This surface process is normally studied for two extreme cases, i.e., SD limited and surface attachment/detachment limited kinetics ("SALK").[13] In this section, we follow the same thread to analyze the inter-facet mass migration between (001) top facet and (111) facet firstly without the external flux. Afterwards, with the external flux, mimicking the practical occasion, the self-limited behavior of facet size is theoretically analyzed. The possibility to employ this behavior to extract useful information (e.g., dominant kinetic process, surface energy ratio, etc.) with trenches of different widths is discussed. It is worthwhile noting that the "WMC"

method treats the individual smooth facet as the basic element of study, rather than dividing into steps and terraces.[10] It captures the main physics and alleviates the burden of computation.

The surface/interface stress will be not taken into consideration for the following discussion, which is believed to also influence the behavior of nano-size particles.[11,12] Additionally, the tapering angle of sidewall is assumed as zero here for the simplicity of the formulas. According to the methodology of "weighted mean curvature,"[13] the average surface chemical potential of facet (001) and facet (111) in Figure 1 can be calculated as

$$\overline{\mu_{001}} = \mu_C + \frac{2\Omega}{L_{001}}\left(\frac{\gamma_{111}}{\sin\theta} - \frac{\gamma_{001}}{\tan\theta}\right) = \mu_C + \frac{2\Omega}{L_{001}} f(\gamma,\theta), \quad (6)$$

$$\begin{aligned}\overline{\mu_{111}} &= \mu_C + \frac{\Omega}{L_{111}}\left[\left(\frac{\gamma_{001}}{\sin\theta} - \frac{\gamma_{111}}{\tan\theta}\right)\right. \\ &\quad \left. + \left(\frac{\gamma_{IIIV-sidewall} - \gamma_{sidewall}}{\cos\theta} - \frac{\gamma_{111}}{\cot\theta}\right)\right] \\ &= \mu_C + \frac{\Omega}{L_{111}} g(\gamma,\theta), \end{aligned} \quad (7)$$

where θ is 54.7° between facet (001) and facet (111). μ_C is the chemical potential of crystal solid phase as reference throughout the discussion of this report. Such facet size dependence of the average chemical potential suggests that the contribution of surface energies of neighboring facets becomes negligible for the larger facet. The extreme case would practically be the blanket substrates. Additionally, the same geometrical relationship as the "Lagrange multiplier" strategy in the case of zero tapering angle can be achieved by equating $\overline{\mu_{001}}$ to $\overline{\mu_{111}}$ for equilibrium.

In order to further investigate the inter-facet migration, we divide the discussion into two extreme cases, i.e., "SD" and "SALK." Physically, for the surface diffusion process, the growth rate is proportional to the second spatial derivative of surface chemical potential. While for the later process, it is linearly proportional to the chemical potential difference in the linear thermodynamic regime (relatively low supersaturation compared to k_BT, *i.e., Boltzmann constant multiplied by temperature*).[19,20] In the following discussion, we construct the surface chemical potential profile with proper assumptions then calculate the migration rate (i.e., growth/recess rate depending on the migration direction) of the two facets for these two extreme cases. However, practically for the MOVPE growth, both processes can be involved in surface kinetics depending on the geometrical size, kinks/steps density, surface temperature, and the kinetic energy barrier of corresponding facet. Finally, we employ the simple decomposition of practical growth rate to assess the possible self-limited behavior of facet size inside trenches when coupling the surface energy driven flux (capillary flux) with external flux for further exploration.

A. Surface diffusion limited case

In this extreme case, the adatoms can be easily attached to/detached from the lattice. Locally, the adatoms can be regarded as equilibrium to the lattice atoms on the facet surface or they have the same chemical potential due to the assumption of fast attachment/detachment step. The surface diffusion step of these adatoms is the limited step to determine the migration rate. Essentially, the adatom diffusion process is driven by the gradient of surface chemical potential based on the second Fick's law, the normal growth rate of the facet induced by surface diffusion is

$$\frac{dz_i}{dt} = \frac{\Omega C_i D_i}{k_B T}\nabla^2\mu, \quad (8)$$

where z_i and t are the normal height of individual facet and growth time, D_i (nm^2/s) and C_i (atoms/nm^2) are, respectively, the surface diffusion constant and areal adatom density of each facet. Ω is the atomic volume (nm^3/atom).[17,18]

Since normally the facet moves parallel to its own plane in submicron trenches, the surface chemical potential of one facet can be constructed to follow a parabolic relationship (the second derivative is constant) because of the same normal (perpendicular to the facet plane) growth rate over the individual facet, i.e., $\mu = ax^2 + bx + c$. To construct the surface chemical potential for each facet, the following conditions should be satisfied:

(1) the surface chemical potential is continuous at the joint of Facet (001) and Facet (111),
(2) the constraint of area or mass conservation, $2GR_{111}^{MIGRATION}L_{111} + GR_{001}^{MIGRATION}L_{001} = 0$, where $GR_{001}^{MIGRATION}$ and $GR_{111}^{MIGRATION}$ are, respectively, the growth/recess rate of Facet (001) and (111) caused by the inter-facet surface migration,
(3) $\frac{\int_{-L_{001}/2}^{L_{001}/2}\mu_{001}(s)ds}{L_{001}} = \overline{\mu_{001}}$, $\frac{\int_0^{L_{111}}\mu_{111}(l)dl}{L_{111}} = \overline{\mu_{111}}$, where s is the distance on Facet (001), l is that on Facet (111),
(4) the flux at the joint of Facet (111) and sidewall is zero due to no exchange of materials with the exterior,
(5) the flux at the middle point of Facet (001) is zero due to the symmetry.

Consequently, the possible surface chemical potential for Facet (001) could be expressed as

$$\begin{aligned}\mu_{100}(s) &= \frac{6(\overline{\mu_{111}} - \overline{\mu_{001}})}{\frac{2D_{001}C_{001}}{D_{111}C_{111}}L_{001}L_{111} + L_{001}^2}\left(s^2 - \frac{L_{001}^2}{12}\right) \\ &\quad + \overline{\mu_{001}}, \left(-\frac{L_{001}}{2} \le s \le \frac{L_{001}}{2}\right), \end{aligned} \quad (9)$$

while for facet (111),

$$\begin{aligned}\mu_{111}(l) &= \frac{3(\overline{\mu_{001}} - \overline{\mu_{111}})}{2L_{111}^2 + \frac{D_{111}C_{111}}{D_{001}C_{001}}L_{001}L_{111}}\left(l^2 - \frac{L_{111}^2}{3}\right) \\ &\quad + \overline{\mu_{111}}, \quad (0 \le l \le L_{111}). \end{aligned} \quad (10)$$

Correspondingly, the growth/recess rate of facet (001) and (111) due to the inter-facet surface diffusion can be obtained as

$$GR_{001}^{MIGRATION} = \frac{12\Omega^2\left[\frac{g(\gamma,\theta)}{L_{111}} - \frac{2f(\gamma,\theta)}{L_{001}}\right]}{k_BT\left(\frac{2L_{001}L_{111}}{D_{111}C_{111}} + \frac{L_{001}^2}{D_{001}C_{001}}\right)}, \quad (11)$$

$$GR_{111}^{MIGRATION} = \frac{6\Omega^2\left[\frac{2f(\gamma,\theta)}{L_{001}} - \frac{g(\gamma,\theta)}{L_{111}}\right]}{k_BT\left(\frac{2L_{111}^2}{D_{111}C_{111}} + \frac{L_{001}L_{111}}{D_{001}C_{001}}\right)}. \quad (12)$$

Equations (11) and (12) suggest that the surface energy, diffusivity and facet size all impact the inter-facet migration progress. The driving force from the surface chemical potential difference is contained in the numerator and the denominator includes the information of surface kinetics. Additionally, if the facet dimension scales with the proportion β, the growth/recess rate scales as β^{-3} in this case of surface diffusion limited kinetics.

B. Surface attachment/detachment limited case

In the case of "SALK," the surface diffusion process is significantly faster compared to the attachment/detachment process to/from kinks or steps, therefore both the adatom and surface chemical potential can be assumed as constant over the whole facet to keep the same normal growth rate, contrary to the parabolic shape in the surface diffusion-limited case. If the linear kinetic coefficients of attachment/detachment processes for (001) and (111) facets are, respectively, k_{001} and k_{111}, the growth/recess rate due to surface energies would be evaluated as

$$GR_{001}^{MIGRATION} = k_{001} * (\tilde{\mu} - \overline{\mu_{001}}), \quad (13)$$

$$GR_{111}^{MIGRATION} = k_{111} * (\tilde{\mu} - \overline{\mu_{111}}) \ . \quad (14)$$

The k_{001} or k_{111} is linear attachment/detachment kinetic coefficient. It depends on the temperature, attachment/detachment energy barrier as well as kink sites density[13,21] and it varies with facets due to different surface atomic configurations. If the facet is growing, the adatoms attach to the kinks/steps, we consider k_{001}/k_{111} as attachment rate accordingly. Otherwise, it represents the detachment rate when the corresponding facet is recessing. $\tilde{\mu}$ is the chemical potential of the ambient phase in which the atoms are exchanging by diffusion. If the desorption process is negligible, this phase is regarded as that of "adsorbed layer." In some cases, $\tilde{\mu}$ is considered as the chemical potential of vapor phase near to the surface, then the limited kinetics will be adsorption/desorption. However, the basic characteristic equations are similar except k_{001} and k_{111} are the adsorption/desorption rate instead.

In the condition of mass conservation $2GR_{111}^{MIGRATION}L_{111} + GR_{001}^{MIGRATION}L_{001} = 0$, the chemical potential of the "adsorbed layer" phase could be calculated as

$$\tilde{\mu} = \frac{2k_{111}L_{111}\overline{\mu_{111}} + k_{001}L_{001}\overline{\mu_{001}}}{2k_{111}L_{111} + k_{001}L_{001}}. \quad (15)$$

Hence,

$$GR_{001}^{MIGRATION} = \frac{\Omega\left[\frac{g(\gamma,\theta)}{L_{111}} - \frac{2f(\gamma,\theta)}{L_{001}}\right]}{\frac{1}{k_{001}}\left(1 + \frac{k_{001}L_{001}}{2k_{111}L_{111}}\right)}, \quad (16)$$

$$GR_{111}^{MIGRATION} = \frac{\Omega\left[\frac{2f(\gamma,\theta)}{L_{001}} - \frac{g(\gamma,\theta)}{L_{111}}\right]}{\frac{1}{k_{111}}\left(1 + \frac{2k_{111}L_{111}}{k_{001}L_{001}}\right)}. \quad (17)$$

Similarly, it is indicating the driving force in the numerator and kinetics in the denominator. But the migration rate scales as β^{-1} different from the "SD" case.

In both limited cases, the migration direction depends on the comparison of $\overline{\mu_{001}}$ to $\overline{\mu_{111}}$. Associated with the average surface chemical potential in Eqs. (6) and (7), if $L_{001}/2L_{111} > f(\gamma,\theta)/g(\gamma,\theta)$, the inter-facet surface migration is from facet (111) to facet (001). The facet size of (001) shrinks by recessing and that of facet (111) expands by growing, in order to reach the equilibrium ratio $f(\gamma,\theta)/g(\gamma,\theta)$. According to Eqs. (11) and (12) for "SD" and (16) and (17) for "SALK," the growth rate of facet (001) and the recess rate of facet (111) versus L_{001} can be calculated in the progression to the ES, schematically shown in Fig. 2. Initially, since the facet size deviates significantly far from the equilibrium value, the migration rate is higher. Afterwards as approaching to the ES (in this case, L_{001} decreases), the driving force is closer to zero and the migration rate drops to zero in both cases without any external supply of atoms. Correspondingly, the opposite case of $L_{001}/2L_{111} < f(\gamma,\theta)/g(\gamma,\theta)$ is also described in the same figure for comparison, where the migration direction is from (001) to (111). Nevertheless, the migration rate follows the same trend.

The growth/recess rate is assessed in this part without any external supply of atoms, only driven by the minimization of total surface energy and limited by the "SD" or "SALK" process. In the following part, we take into consideration the external supply of atom flux during the MOVPE growth.

C. Analysis with external arriving flux

During the process of epitaxy, the atoms arrive to the facet surface externally. The contribution to the observed growth rate of individual facet could be divided into external atoms and inter-facet migrating atoms, as shown in Fig. 3(a). It could be approximated as the isolated growth rate modified by the inter-facet migration induced by surface energy, as treated in Refs. 11, 12, and 14. To stabilize the crystal profile,[11,12,22] it is necessary that the ratio of growth rate of (111) to (001) is $\cos\theta$ (in this case, 0.5779), as illustrated in Fig. 3(b). This statement can be expressed as

$$\frac{GR_{111}^{ISOLATED} + GR_{111}^{MIGRATION}}{GR_{001}^{ISOLATED} + GR_{001}^{MIGRATION}} = \cos\theta, \quad (18)$$

where $GR_{001}^{ISOLATED}$ and $GR_{111}^{ISOLATED}$ are the growth rates of (001) and (111) facet, respectively, without the inter-facet

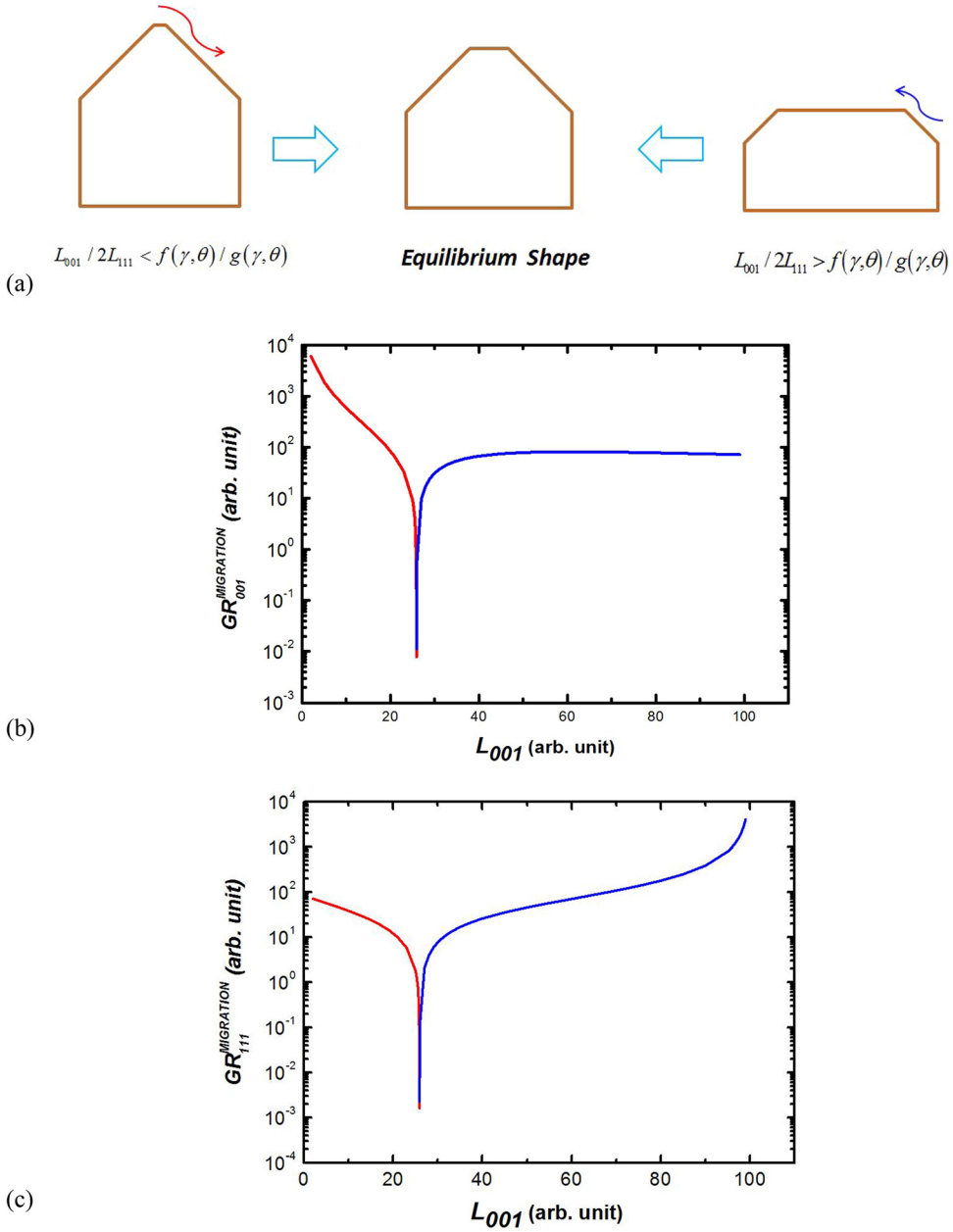

FIG. 2. (a) Schematic of two possible migration direction, (b) the growth/recess rate of Facet (001) for the inter-facet migration, (c) the growth/recess rate of Facet (111) for the inter-facet migration, red line: from (001) to (111), blue line: from (111) to (001). Both of them reach to the equilibrium shape eventually with dropping growth rate.

migration. It suggests the amount of materials per area can be effectively deposited onto the facets, which is determined primarily by the vapor phase diffusion and surface reaction kinetics in the occasion of MOVPE (e.g., the cracking efficiency of precursors, absorption/desorption). Associated with the geometrical requirement $2L_{111}\cos\theta + L_{001} = W$ and mass conservation, the stable shape (e.g., L_{001}^{stable} and L_{111}^{stable}) should satisfy in different trenches

$$GR_{111}^{ISOLATED} - GR_{001}^{ISOLATED}\cos\theta = \frac{W}{2L_{111}^{stable}} GR_{001}^{MIGRATION}. \tag{19}$$

The solution to this equation, might achieved numerically, indicates the stable length of (001) and (111) facet inside trenches for specific growth conditions. Practically, the limited information of surface energies, diffusion barrier energy/attachment rate, etc., during the growth hinders the quantitative delineation of facet evolution inside sub-micron trenches. Thereby, the theoretical analysis based on the modified expressions could be feasible with the measurement of stable facet sizes. For the "SD" case,

$$\frac{\left(L_{111}^{stable}L_{001}^{stable}\right)^2}{W} = \frac{6\Omega^2 g(\gamma,\theta) D_{001}C_{001}}{k_B T\left(GR_{111}^{ISOLATED} - GR_{001}^{ISOLATED}\cos\theta\right)} \times \left[\frac{\frac{L_{001}^{stable}}{2L_{111}^{stable}} - \frac{f(\gamma,\theta)}{g(\gamma,\theta)}}{\frac{L_{001}^{stable}}{2L_{111}^{stable}} + \frac{D_{001}C_{001}}{D_{111}C_{111}}}\right]. \tag{20}$$

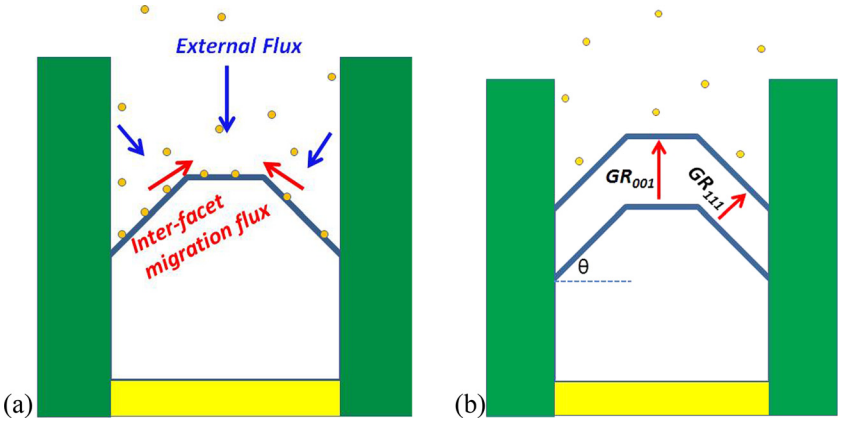

FIG. 3. (a) Schematic of two components of flux contributing the individual facet growth rate, in this case, adatoms migrate from (111) to (001), (b) stabilization of facet size when the growth rate ratio is equivalent to $\cos\theta$.

If the "SALK" process dominates, the followed expression can be obtained:

$$\frac{L_{111}^{stable}L_{001}^{stable}}{W} = \frac{\Omega g(\gamma,\theta)k_{111}}{\left(GR_{111}^{ISOLATED} - GR_{001}^{ISOLATED}\cos\theta\right)} \times \left[\frac{\frac{L_{001}^{stable}}{2L_{111}^{stable}} - \frac{f(\gamma,\theta)}{g(\gamma,\theta)}}{\frac{L_{001}^{stable}}{2L_{111}^{stable}} + \frac{k_{111}}{k_{001}}}\right]. \quad (21)$$

First of all, we notice that the exponent n of $\left(L_{111}^{stable}L_{001}^{stable}\right)^n/W$ is 2 for the "SD" case and 1 for the "SALK" case, respectively. Such difference could provide justification of which surface process dominates via proper mathematical fitting for practical applications. Furthermore, depending on the comparison of $GR_{001}^{ISOLATED}\cos\theta$ to $GR_{111}^{ISOLATED}$, there can be three cases,

(1) $GR_{111}^{ISOLATED} = GR_{001}^{ISOLATED}\cos\theta$, the stable facet size should satisfy $L_{001}^{stable}/2L_{111}^{stable} = f(\gamma,\theta)/g(\gamma,\theta)$, just similar to the equilibrium occasion,
(2) $GR_{111}^{ISOLATED} < GR_{001}^{ISOLATED}\cos\theta$, the stable size should follow $L_{001}^{stable}/2L_{111}^{stable} < f(\gamma,\theta)/g(\gamma,\theta)$, now the $\left(L_{111}^{stable}L_{001}^{stable}\right)^n/W$ is a decreasing function of $L_{001}^{stable}/2L_{111}^{stable}$ for trenches of different widths,
(3) $GR_{111}^{ISOLATED} > GR_{001}^{ISOLATED}\cos\theta$, the stable size should follow $L_{001}^{stable}/2L_{111}^{stable} > f(\gamma,\theta)/g(\gamma,\theta)$, instead the $\left(L_{111}^{stable}L_{001}^{stable}\right)^n/W$ is an increasing function of $L_{001}^{stable}/2L_{111}^{stable}$ for different trenches. Mathematically, it has an asymptotic value of C_{SD} or C_{SALK},

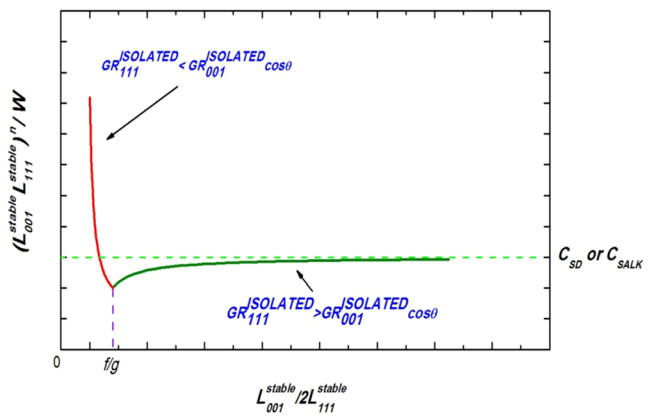

FIG. 4. Schematic of $\left(L_{111}^{stable}L_{001}^{stable}\right)^n/W$ versus $L_{001}^{stable}/2L_{111}^{stable}$ in trenches of different widths for three different possible cases. n = 2 for "SD" case and n = 1 for "SALK."

where we define the coefficients as followed

$$C_{SD} = \frac{6\Omega^2 g(\gamma,\theta)D_{001}C_{001}}{k_BT\left|GR_{111}^{ISOLATED} - GR_{001}^{ISOLATED}\cos\theta\right|},$$

for the case of ''SD'',

$$C_{SALK} = \frac{\Omega g(\gamma,\theta)k_{111}}{\left|GR_{111}^{ISOLATED} - GR_{001}^{ISOLATED}\cos\theta\right|},$$

for the case of ''SALK''.

All of them are summarized schematically in Fig. 4.

Finally, proper mathematical curve fitting could theoretically obtain the value of $f(\gamma,\theta)/g(\gamma,\theta)$, and $D_{001}C_{001}/D_{111}C_{111}$ or k_{111}/k_{001} based on the data from different trench widths. However, during the selective growth inside submicron trenches, the difference between the supply of materials to facet (001) and facet (111) could be influenced by the geometry in terms of vapor phase diffusion, which could be potentially influenced by the trench size. Hence, the isolated growth rate of facets and furthermore the coefficient C_{SD} or C_{SALK} could be different for variant trench width. Nevertheless, the ratio $\left(L_{111}^{stable}L_{001}^{stable}\right)^n/W$ will approach to the extreme for the shrinking trench dimension. Accordingly, the ratio $L_{001}^{stable}/2L_{111}^{stable}$ theoretically approaches to the value of $f(\gamma,\theta)/g(\gamma,\theta)$.

IV. CONCLUSION

In summary, we analyzed the evolution of crystal shape inside submicron trenches in the case of (001) and (111) facets with surface/interface energy considered. The equilibrium shape is reached when $L_{001}/2L_{111}$ equals $f(\gamma,\theta)/g(\gamma,\theta)$. In the non-equilibrium case, the growth/recess rate of corresponding facet induced by inter-facet migration is explicitly modeled based on the "WMC" method in both the "SD" and "SALK" cases. Coupled with the external flux, the self-limited behavior of facet size is theoretically predicted with the relationship of

$\left(L_{111}^{stable}L_{001}^{stable}\right)^n/W$ versus $L_{001}^{stable}/2L_{111}^{stable}$ acquired. n = 2 indicates the "SD" regime and n = 1 the "SALK" regime. Three different cases can be categorized according to the comparison of $GR_{001}^{ISOLATED}\cos\theta$ to $GR_{111}^{ISOLATED}$. Further work is needed to investigate the impact of external flux on the adatom density (chemical potential) on the facets with the joint consideration of two kinetics and the involvement of surface/bulk strain energy for nano-trenches.

ACKNOWLEDGMENTS

This work is supported by IMEC Industrial Affiliation Program. The present authors would like to thank the Logic Program and Management, partners.

[1]H. Hirayama, M. Hiroi, and T. Ide, Phys. Rev. B **48**, 17331 (1993).
[2]T. Aoyama, T. Ikarashi, K. Miyanaga, and T. Tatsumi, J. Cryst. Growth **136**, 349 (1994).
[3]L. Vescan, K. Grimm, and C. Dieker, J. Vac. Sci. Technol. B **16**, 1549 (1998).
[4]G. Wang, M. R. Leys, N. D. Nguyen, R. Loo, G. Brammertz, O. Richard, H. Bender, J. Dekoster, M. Meuris, M. M. Heyns, and M. Caymax, J. Electrochem. Soc. **157**, H1023 (2010).
[5]C. Merckling, N. Waldron, S. Jiang, W. Guo, O. Richard, B. Douhard, A. Moussa, D. Vanhaeren, H. Bender, N. Collaert, M. Heyns, A. Thean, M. Caymax, and W. Vandervorst, J. Appl. Phys. **114**, 033708 (2013).
[6]T. Sato, I. Tamai, and H. Hasegawa, J. Vac. Sci. Technol. B **22**, 2266 (2004).
[7]S. Koshiba, Y. Nakamura, M. Tsuchiya, H. Noge, H. Kano, Y. Nagamune, T. Noda, and H. Sakaki, J. Appl. Phys. **76**, 4138 (1994).
[8]S. Guha and A. Madhukar, J. Appl. Phys. **73**, 8662 (1993).
[9]M. Ozdemir and A. Zangwill, J. Vac. Sci. Technol. A **10**, 684 (1992).
[10]M. Ozdemir and A. Zangwill, Phys. Rev. B **45**, 3718 (1992).
[11]G. Biasiol and E. Kapon, Phys. Rev. Lett. **81**, 2962 (1998).
[12]G. Biasiol, A. Gustafsson, K. Leifer, and E. Kapon, Phys. Rev. B **65**, 205306 (2002).
[13]W. C. Carter, A. R. Roosen, J. W. Cahn, and J. E. Taylor, Acta Metall. Mater. **43**, 4309 (1995).
[14]V. B. Shenoy, J. Mech. Phys. Solids **59**, 1121 (2011).
[15]J. E. Taylor, J. W. Cahn, and C. A. Handwerker, Acta Metall. Mater. **40**, 1443 (1992).
[16]J. E. Taylor, Acta Metall. Mater. **40**, 1475 (1992).
[17]W. W. Mullins, J. Appl. Phys. **28**, 333 (1957).
[18]W. W. Mullins, Interface Sci. **9**, 9 (2001).
[19]D. Kondepudi and I. Prigogine, *Modern Thermodynamics: From Heat Engines to Dissipative Structures* (John Wiley & Sons Ltd., West Sussex, 1998).
[20]H. Spohn, J. Phys. I France **3**, 69 (1993).
[21]H. C. Jeong and E. D. Williams, Surf. Sci. Rep. **34**, 171 (1999).
[22]E. Pelucchi, V. Dimastrodonato, A. Rudra, K. Leifer, E. Kapon, L. Bethke, P. A. Zestanakis, and D. D. Vvedensky, Phys. Rev. B **83**, 205409 (2011).